JBC Papers in Press. Published on June 21, 2002 as Manuscript M110714200

Characterization and channel coupling of the $P2Y_{12}$ nucleotide receptor of brain capillary endothelial cells

Joseph Simon‡, Alexander K. Filippov¶, Sara Göransson‡, Yung H. Wong+, Christian Frelinƒ, Anton D. Michel#, David A. Brown¶ and Eric A. Barnard‡§

From the ‡Department of Pharmacology, and the #Glaxo Institute of Applied Pharmacology, University of Cambridge, Tennis Court Road, Cambridge CB2 1PD, UK, the ¶Department of Pharmacology, University College London, Gower Street, London WC1E 6BT, UK, the +Department of Biochemistry, Hong Kong University of Science and Technology, Clear Water Bay Road, Hong Kong, China and the ƒInstitut de Pharmacologie Moleculaire et Cellulaire, CNRS UMR6097, 660 Route des Lucioles, Sophia Antipolis, 06560 Valbonne, France

Running title: $P2Y_{12}$ receptor of brain capillary endothelial cells

§To whom correspondence should be addressed: Department of Pharmacology, University of Cambridge, Tennis Court Road, Cambridge CB2

1PD, UK; Tel: +44 1223 847876; Fax: +44 1223 843090; E-mail:

eb247@cam.ac.uk

[**SUMMARY**]

Rat brain capillary endothelial (B10) cells express an unidentified nucleotide receptor linked to adenylyl cyclase inhibition. We show that this receptor in B10 cells is identical in sequence to the $P2Y_{12}$ ADP receptor ("*P2Y$_T$*") of platelets. When expressed heterologously, 2-methylthioADP (2-MeSADP; EC_{50}: 2 nM), ADP and ADPβS were agonists of cyclic-AMP decrease and 2-propylthio-D-β,γ-difluoromethyleneATP (AR-C66096) was a competitive antagonist (K_B: 28 nM), as in platelets. However, 2-MeSATP (EC_{50}: 0.4 nM), ATP (1.9 μM) and 2-chloroATP (190 nM), antagonists in the platelet, were also agonists. 2-MeSADP activated (EC_{50}: 0.1 nM) GIRK1/GIRK2 inward rectifier K^+ channels when co-expressed with $P2Y_{12}$ receptors in sympathetic neurons. Surprisingly, $P2Y_1$ receptors expressed likewise gave that response, however, a full inactivation followed, absent with $P2Y_{12}$ receptors. A new $P2Y_{12}$-mediated transduction was found, the closing of native N-type Ca^{2+} channels; again both 2-MeSATP and 2-MeSADP are agonists (EC_{50}: 0.04 and 0.1 nM, respectively). That action, like their cyclic-AMP response, was pertussis toxin-sensitive. The Ca^{2+} channel inhibition and K^+ channel activation are mediated

by βγ-subunit release from a heterotrimeric G-protein. Gα subunit types in B10 cells were also identified. The presence in the brain capillary endothelial cell of the $P2Y_{12}$ receptor is a significant extension of its functional range.

Keywords: $P2Y_{12}$ receptor; adenine nucleotides; brain capillary endothelial cell; platelets; adenylyl cyclase inhibition; inward rectifier, N-type Ca^{2+}-channel.

B10 cells are an endothelial clonal line derived spontaneously by culture and selection of rat brain microvascular endothelial cells (1), a source of considerable pharmacological potential. The B10 cells respond to extracellular adenine (but not uracil) nucleotides with intracellular Ca^{2+} mobilization, mediated by a G-protein-coupled $P2Y_1$ receptor (2). While the known rat $P2Y_1$ receptor cDNA could be isolated from the B10 cells (2), no transcript for any other then-known P2Y receptor subtype was detectable in them. However, the B10 cells were found to exhibit another second messenger response, namely the inhibition of stimulated adenylyl cyclase, but with a nucleotide agonist specificity very similar to that of the $P2Y_1$ receptor (2). It was further demonstrated (3) that selective antagonists of the $P2Y_1$ receptor such as adenosine-3'-phosphate-5'-phosphate (A3P5P) were unable to affect that response, while it showed high sensitivity to 2-propylthio-D-

β,γdifluoromethyleneATP (AR-C66096), a specific antagonist (4, 5) of the adenylyl cyclase-inhibitory *P2Y$_T$* or "P2T" receptor for ADP, which was known as an important functional component of blood platelets. That study (3) demonstrated that a second P2Y receptor activity is present in the B10 cell, with some of its functional features in common with the platelet *P2Y$_T$* receptor.

Recently, a cDNA encoding a nucleotide receptor with a novel seven-transmembrane sequence was identified independently by two groups, starting from a human platelet cDNA library or an orphan human DNA sequence, and shown to be distantly but significantly related to the known P2Y receptors (6, 7). This was designated as the P2Y$_{12}$ receptor. Its amino acid sequence lies on a hitherto-unrecognised separate branch of the P2Y family (8). It was characterized in both studies to show its adenine nucleotide specificity and its inhibition of forskolin-stimulated adenylyl cyclase, in which it corresponds to the platelet *P2Y$_T$* receptor (6, 7). That human P2Y$_{12}$ receptor cDNA was expressed again in cell line hosts by other groups, confirming the reported series of agonists but with higher potencies in the cAMP decrease (9) and showing their affinities by competition with the binding of radiolabeled 2-MeSADP (9,10). In the original identification of the human P2Y$_{12}$ receptor a similar cDNA was also derived from a rat platelet library (6) and its RNA was shown to express in *Xenopus* oocytes, but this receptor was not further characterized.

The question, therefore, obviously arises as to whether the cyclase-inhibitory receptor for adenine nucleotides of the B10 capillary endothelial cell

is in fact the $P2Y_{12}$ receptor. However, this cannot necessarily be assumed, since the "P2T" receptor has commonly been described in the literature as specific to the platelet (see reviews: 11, 12). Further, the adenylyl cyclase-inhibitory P2Y receptor activity in the B10 cell differs in an important respect from that in the platelet, namely in the response to the nucleotide triphosphates: in B10 cells (3) ATP and 2-ClATP are weak partial agonists and 2-MeSATP is a very potent full agonist (EC_{50}: 3.5 nM), whereas in the platelet these and other adenosine triphosphates are antagonists (13,14). It may be, therefore, that these endothelial cells contain a different subtype related to the $P2Y_{12}$ receptor, or even a quite different, hitherto unknown receptor of the P2Y family, while yet other explanations are also possible (3). This has remained as an outstanding question in our knowledge of the P2Y family.

We have, therefore, screened the B10 cell mRNA population for sequences related to the platelet $P2Y_{12}$ receptor, and show that it is the authentic platelet $P2Y_{12}$ receptor sequence which is present. The pharmacological properties of the rat $P2Y_{12}$ receptor have been characterized and their relationship to the B10 cell phenotype are discussed. Those properties include two primary $P2Y_{12}$ transductions, the direct activation of a G-protein-coupled inward rectifier K^+ (GIRK) channel and the direct closing of a voltage-gated N-type Ca^{2+} channel (Ca^{2+}_N channel).

EXPERIMENTAL PROCEDURES

Materials:

All media and reagents for cell culture were purchased from Life Technologies. ATP, ADP, adenosine 5'-*O*-(2-thio)diphosphate (ADP^2S), hexokinase and all restriction enzymes used were from Roche Molecular Biochemicals. 2-MethylthioATP (2-MeSATP), 2-methylthioADP (2-MeSADP), 2-chloroATP (2-ClATP), 2&3-*O*-(4-benzoylbenzoyl)-adenosine 5-triphosphate (BzATP), creatine phosphate, creatine phosphokinase, 3-isobutyl-1-methylxanthine (IBMX), cyclicAMP (cAMP), forskolin, protein kinase A (PKA: cAMP-binding regulatory subunit) and pertussis toxin were from Sigma. RNA isolation kit and RNase- free DNase I were from Stratagene. TA Cloning Kit and pcDNA 3.1(+) plasmid were from Invitrogen. 2-propylthio-D-β,γdifluoromethyleneATP (AR-C66096) was the sample synthesized previously (3). Antisera against G-protein subunits were purchased from the following suppliers: antiserum Go/1 (for $G\alpha_o$), EC/2 (for $G\alpha_{i3}$), AS/7 (for $G\alpha_{i1}$ and $G\alpha_{i2}$) and RM/1 (for $G\alpha_s$ and $G\alpha_{olf}$) from Perkin-Elmer Life Sciences - NEN; antisera S-20 (for $G\alpha_{12}$), A-20 (for $G\alpha_{13}$) and C-16 (for $G\beta_1$) from Santa Cruz Biotechnology; antisera 371727 (for $G\alpha_{i2}$), 371754 (for $G\alpha_q$ and $G\alpha_{11}$), 371783 (for $G\alpha_{16}$) from Calbiochem-Novabiochem; antisera PC64 (for $G\alpha_z$), G51829 (for $G\alpha_{t1}$) 3A-195 ($G\alpha_{14}$) from Oncogene Research Products, Transduction Laboratories and Gramsch Laboratories, respectively. [2,8-^{3}H]-adenosine 35-cyclic monophosphate ([^{3}H]-cAMP: 25-40 Ci/mmol), the secondary antibodies used and the ECL chemoluminescence detection kit

were from Amersham Pharmacia Biotech. All other chemicals were of analytical grades from established commercial sources.

The purity of all nucleotides used in this study was assured by the use of enzymic regeneration systems as described previously (3). Thus, all adenosine diphosphate stock solutions (1 mM) were treated with 10 U/ml hexokinase/25 mM glucose/2 mM $MgCl_2$ to convert any triphosphate contaminations to diphosphates. Any diphosphate contamination of adenosine triphosphates was eliminated by creatine phosphokinase/creatine phosphate treatment (3). The treated drug solutions were then used in adenylyl cyclase assays or in electrophysiological measurements.

1321N1 astrocytoma and Chinese hamster ovary (CHO-K1) cells were originally from the European Collection of Animal Cell Cultures.

Isolation of cDNA encoding the P2Y$_{12}$ receptor:

B10 cells (subclone **a** as in ref. 3) were cultured to confluency and harvested by trypsinization. Total RNA from these cells was extracted using a micro RNA isolation kit (Stratagene), and was treated with RNase-free DNase I for 30 min at 37^{o}C. First-strand cDNA was synthesized (60 min, 42^{o}C, 100µl reaction volume) from 10 µg of total RNA using oligo(dT)$_{18}$ primer and Moloney murine leukemia virus reverse transcriptase (First Strand Synthesis Kit, Clontech). Primers based on the recently cloned rat platelet P2Y$_{12}$ cDNA sequence (Genbank accession number: AF313450) were designed to amplify the entire coding sequence of such receptors by polymerase chain reaction (PCR): 5-

AGAATAACCAGGACCATGGAGGTG-3 (forward); 5ATTCTACAT TGGGGTCTCCTCGCT-3 (reverse). PCR amplifications were performed on 2 μl of first-strand reaction product using the forward and reverse primers (200 ng each), deoxynucleotides (each at 200 μM), 1.5 mM $MgCl_2$ in the presence of 2.5 units of Dynazyme DNA polymerase (Flowgen). Cycling parameters were: 94^{o}C, 1 min, 55^{o}C, 1 min, 72^{o}C, 2 min for 30 cycles, with a final extension at 72^{o}C for 10 min. The resulting single PCR product of 1050 bp was cloned into pCR 2.1 vector (TA Cloning kit, Invitrogen). Ten clones were sequenced completely using an automated DNA sequencer and were identical. For functional expression, the rat $P2Y_{12}$ cDNA was subcloned into the pcDNA 3.1(+) mammalian expression vector (Invitrogen) at the Hind III-Xho I sites to give the correct orientation for transcription. The identity and orientation of the resulting clones were also verified by sequencing.

The cDNA sequence of the human $P2Y_{12}$ receptor (Genbank: AF313449) was also used to design PCR primers equivalent to those used for the rat. Using human genomic DNA as the source, identical methods were applied to obtain for comparison the human $P2Y_{12}$ cDNA inserted into the pcDNA 3.1(+) vector.

Heterologous expression and selection:

$1x10^6$ wild-type 1321N1 astrocytoma cells were transfected with 4 μg of the rat $P2Y_{12}$-pcDNA 3.1(+) plasmid construct by electroporation (Easy-Ject,

EquiBio, Kent, UK). Transfected cells were selected in Dulbeccos modified Eagles medium (DMEM)/Nutrient mix F-12 supplemented with Glutamax-1, pyridoxine, 10% fetal bovine serum (culture medium) plus 600 μg/ml geneticin sulfate (G418) for stable expression of the rat $P2Y_{12}$ receptor. Cells were maintained in the above medium at 37^{o}C in a humidified atmosphere (95% air, 5% CO_2) and passaged by trypsinization every 4-5 days. For the adenylyl cyclase assays, the cells stably expressing the rat $P2Y_{12}$ receptor were plated on flat-bottom polystyrene 96-well-tissue culture plates (at ~25,000 cells per well) and were grown to near confluency.

The human $P2Y_{12}$ plasmid construct was similarly transfected into CHO-K1 cells, selected for stable expression as described above and prepared likewise for adenylyl cyclase assays.

Adenylyl cyclase assay:

The measurements were performed as we recently described in 96-well plates (3), using the method based on competition for the binding of cyclic [^{3}H]-AMP to a binding fragment of protein kinase A (15). Confluent layers of cells heterologously expressing the $P2Y_{12}$ (rat or human) receptor were washed with serum-free culture medium containing 25 mM HEPES and 5 mM glucose, pH7.4 at 37^{o}C and then pre-incubated in the same medium containing 200 μM IBMX for 15 min at 37^{o}C (to inhibit breakdown of cyclic AMP by phosphodiesterases). Incubations with effectors (as stated each case here)

were made in the presence of 10 μM forskolin and 200 μM IBMX for 5 min at 37^{o}C. Control experiments performed on 1321N1 or CHO-K1 cells transfected similarly but with vector alone gave no detectable decrease in the stimulated cyclic AMP (cAMP) level.

For antagonism studies, the cells were pre-incubated with AR-C66096 or BzATP at the stated concentrations for 15 min at 37^{o}C in medium containing 200 μM IBMX; then the stated concentrations of 2-MeSADP as agonist were each added, plus forskolin to 10 μM, for a further 5 min incubation at 37^{o}C. For pertussis toxin treatment, the 1321N1 cells stably expressing the recombinant rat $P2Y_{12}$ receptor were cultured on 96-well plates to near confluency. Half of the wells on each plate were incubated with 100 ng/ml pertussis toxin and the other half without, in culture medium with G418 at 37^{o}C for 14 -16 h, before use in experiments.

Analysis of G-protein subunits in B10 and 1321N1 cells:

Cells were grown to confluency, harvested in phosphate-buffered saline (PBS) containing 10 mM EDTA. Cells were collected by centrifugation (200 x g, 5 min, 4^{o}C) and resuspended in 2 ml ice-cold hypotonic lysis buffer (50 mM Tris-HCl, pH 7.5, 2.5 mM $MgCl_2$, 1 mM EGTA, 1 mM dithiothrietol (DTT), 0.1 mM phenylmethylsulfonyl fluoride (PMSF), 1 mM benzamidine-HCl) and homogenized by freeze-thaw and 10 passages through a 27-gauge needle. The homogenate was centrifuged for 5 min at 200 x g, the pellet was discarded

and the plasma membrane fraction collected by centrifugation at 15,000 x g for 30 min. The pellet was finally resuspended in hypotonic lysis buffer and its protein concentration was measured (DC Protein Assay Kit, Bio-Rad Laboratories). Membrane proteins (50 μg per lane) were separated on a 12.5 % SDS polyacrylamide gel and the bands were electro-blotted onto nitrocellulose membranes. Immunodetection of various Gα subunits on the blots were achieved using standard techniques, with a large excess of the specific antisera against $G\alpha_o$ and $G\beta_1$ subunits that are detailed in the Materials section. Horseradish peroxidase-(HRP)-conjugated IgG was applied as the secondary antibody. The signals were detected by ECL-chemoluminescence.

Injections of rat superior cervical ganglion (SCG) neurons and electrophysiological recordings:

Isolation of SCG neurons and injection of plasmids were as previously (16,17). Briefly, the SCG neurons isolated from 15-19 day-old rats were plated on coverslips 4-6 h prior to DNA micro-injection into the cell nucleus. The cells were co-injected with the rat $P2Y_{12}$–pcDNA 3.1(+) plasmid (100 ng/μl) and the enhanced Green Fluorescent Protein (EGFP, S65T mutant; Clontech) cDNA in pcDNA 3 vector (25 ng/μl). For the modulation of the inwardly rectifying K^+ current, GIRK1 and GIRK2 cDNAs in pcDNA 3 (100 ng/μl each; generous gifts from Dr. F. Lesage) were also present in the injection buffer. The injected neurons were then cultured at 37^{o}C for 14-24 h prior to electrophysiological

recordings.

The agonist was applied to the cells in a constantly perfusing solution (bath exchange $\leq$ 2 s): this avoids any degradation of the agonist due to enzymic action at the surface of the cells. Whole-cell currents through the GIRK channels in fluorescent cells were recorded as described (18) but at ~20 ^{o}C, in perforated patch mode, with external KCl 6 mM and with a 200-ms range for the standard ramp voltage commands applied. Currents through the N-type Ca^{2+} channels carried by 5 mM Ba^{2+} were recorded and identified as described previously (19). The currents were routinely evoked every 20 s, for a period of 50 ms, by a depolarizing test pulse from –90 mV to 0 mV; they are shown as leak-corrected by subtracting the current remaining after substituting 5 mM Co^{2+} for Ba^{2+} in the external solution (as illustrated in ref.16). Pertussis toxin incubation here was at 500 ng/ml, 24 h, starting 1h after plasmid injection of the cells. Other methods, including ensuring and maintaining nucleotide purity, were as before (16, 17).

Data analysis:

At least three independent replicate experiments, each in triplicate, were performed in all adenylyl cyclase assays to give the values reported, represented as the mean±s.e.mean. Agonist concentration-response curves were computer-fitted to a simple logistic equation and the EC_{50} values, referring to the agonist action (inhibition) of nucleotides on the stimulated adenylyl cyclase activity, were calculated using GraphPad Prism (GraphPad

Software). pK_B values for antagonists were obtained from Schild plots of such fitted data. For electrophysiological experiments, a concentration-response data set was obtained from each of at least 3-5 cells. Curves were then fitted (using Origin 5.0 Software) to pooled mean data points using the Hill equation $y=y_{max}x^{nH}/(x^{nH}+K^{nH})$, where y = % of change in current, y_{max}= extrapolated maximum change, x= ligand concentration (nM), K= EC_{50} of the agonist (nM) and n_H= Hill coefficient.

RESULTS

Cloning and sequence analysis of the $P2Y_T$ receptor from B10 cells:

Forward and reverse oligonucleotide primers (see Methods) based on the known $P2Y_{12}$ receptor sequence (6) from platelets were designed to amplify the full coding region. A single product of 1050 bp was obtained by RT-PCR with this primer set using mRNA from B10 cells. This DNA sequence contains an open reading frame of 1029 bp encoding 343 amino acid residues (Fig. 1). It is identical to the deposited Genbank rat receptor sequence (AF313450).

Dendrograms of human P2Y receptor protein sequences (7, 8) had shown that the $P2Y_{12}$ sequence is very divergent from the others, being on a distinct second branch with the UDP-glucose receptor. The next closest, although still

quite low in shared identity, is the sequence (human) of the $P2Y_5$ receptor (which gives some response to ATP in oocyte expression (20)). A dendrogram of rat P2Y receptor sequences (where known) shows the same separation (not shown). However, the rat $P2Y_{12}$ receptor shares 85 % sequence identity with the human $P2Y_{12}$ receptor and they are clearly orthologues (Fig.1). 49 amino acids are changed between them. These changes are concentrated in the N- and C-termini and in the 3rd intracellular loop. In addition to these changes, there are 6 amino acid additions into the N-terminal region, plus a 5-residue deletion in the C-terminal, of the human receptor (Fig. 1). Some differences in properties might therefore be expected.

Heterologous expression and pharmacology of the recombinant $P2Y_T$ receptor of B10 cells:

The identified cDNA in pcDNA 3.1(+) mammalian expression vector was transfected into 1321N1 astrocytoma cells and a stably-expressing cell line was selected. The effects of various nucleotides on the cAMP level were determined. When these cells were transfected with the host vector alone, none of the nucleotides applied had an effect on the cAMP level, either basal or after its elevation by 10 μM forskolin (data not shown). 2-MeSATP or 2-MeSADP, which were shown to be potent agonists at the *$P2Y_T$* receptor in B10 cells (3), inhibited the forskolin-stimulated adenylyl cyclase in a dose-dependent manner (Fig. 2). The maximum inhibition of the stimulated adenylyl cyclase activity was about 50 % in all cases (Figs. 2, 3 and 4). They were

potent full agonists here (Table 1). ADP and ADPβS were also agonists but with lower potencies (Fig. 2). Other triphosphates such as 2-ClATP and ATP were also full agonists here (Fig 2 and Table 1), in contrast to their antagonistic behavior on platelets (14) or partial agonism on B10 cells (3). The rank order of agonist potencies here is: 2-MeSATP>2-MeSADP >ADP >ADPβS>2-ClATP>ATP. Their potencies are very similar to the values found for the recombinant human $P2Y_{12}$ receptor cloned from genomic DNA in our laboratory, heterologously expressed in CHO cells and assayed in identical conditions (Table 1). The ratios of the potencies in that series do not differ significantly between the two sets, indicating no difference between the two species with these agonists. However, these potencies for the human receptor in CHO-K1 cells are 3.5 - 8 fold higher (except for ADP and ADPβS) than the values recently published by Zhang *et al.* (7) for the same reaction, also with the recombinant human $P2Y_{12}$ receptor in CHO cells, when the same agonists are compared (Table 1). The differences could be explained by a higher expression level in our case of both the rat and human $P2Y_{12}$ receptors.

In the 1321N1 astrocytoma cells heterologously expressing the $P2Y_{12}$ receptor of B10 cells, the inhibition induced by 2-MeSADP of stimulated adenylyl cyclase activity was potently and competitively antagonized (Fig. 3A) by AR-C66096, a selective antagonist of the platelet *$P2Y_T$* (P2T) receptor (4). The K_B value here is 28 nM. As we recently found for B10 cells (3), so here on 1321N1 cells heterologously expressing the $P2Y_{12}$ receptor cloned from those

cells, BzATP is also a competitive antagonist of the 2-MeSADP-evoked inhibition of cAMP accumulation (K_B: 9 μM, Fig. 3B). These K_B values are in good agreement with the values found in B10 cells for the same antagonists, (Table 1). In contrast the $P2Y_1$ receptor selective antagonist A2P5P, even at 100 μM concentration, gave no reduction of the 2-MeSADP-induced inhibition of cAMP accumulation (data not shown).

As in B10 cells (3), treatment here with pertussis toxin (100 ng/ml, 16 h) completely abolished the 2-MeSADP-evoked inhibition of stimulated adenylyl cyclase activity (Fig. 4). Hence, upon agonist activation the recombinant rat $P2Y_{12}$ receptor couples though members of the G_i/G_o family of G-proteins to inhibit adenylyl cyclase.

Availability of G-proteins in B10 and 1321N1 cells:

In view of the latter finding, we investigated the availability of different Gα subunits in native B10 and in 1321N1 host cells. Western blot analysis of B10 cell membranes with antibodies selective for different Gα subunits gave consistent results in multiple determinations, with representative blots shown in Fig. 5. They revealed that all 3 $G\alpha_i$ subtypes are present (Fig. 5A). The $G\alpha_{i2}$ subtype is at distinctly lower density than the other $G\alpha_i$ subunits. The $G\alpha_o$ subunit (which is less common outside the nervous system) is also present (Fig. 5A). $G\alpha_{i2}$ and $G\alpha_{i3}$ and possibly $G\alpha_{i1}$, as well as $G\alpha_o$, are also present in the 1321N1 astrocytoma cell line used as a host for the heterologous

expression of the recombinant rat $P2Y_{12}$ receptor (Fig. 5B).

An alternative possibility would be coupling through $G\alpha_z$, also linked to adenylyl cyclase inhibition (21) and active in the platelet (22), but that case can be eliminated since the $G\alpha_z$ subunit is absent in both B10 and 1321N1 cells (Fig. 5A,B).

$G\alpha_S$ is also present but in low density in B10 cells (Fig. 5A). One $G\beta$ subunit was studied, β_1, which is well represented in both cell lines (Fig. 5A and B). As expected the $G\alpha_{q/11}$ subunits are also seen in both cell lines (Fig. 5A and B), in line with their coupling to the Ca^{2+}-mobilizing $P2Y_1$ receptor, a reaction shown to occur endogeneously in B10 cells (2) and when that receptor is expressed heterologously in 1321N1 cells.

Coupling of the $P2Y_{12}$ receptor to inward rectifier K^+ channels:

The receptor was expressed heterologously by micro-injection of its plasmid DNA into freshly-isolated SCG neurons as host cells, followed by patch-clamping. For revealing receptor/channel couplings, this system, as we have previously shown with other P2Y subtypes (16, 17, 19, 23), has advantages over the usual transfection of immortalized cell lines: only the expressing cells are recorded and coupling through endogenous ion channels in a native neuron can be analyzed. Further, at the stage at which these cells are used there is no significant expression of endogeneous P2Y receptors (16, 17),

native $P2Y_{12}$ receptors there also now being excluded by the controls shown in Fig. 6A. We also extended here its application to P2Y receptors by co-expressing an inward rectifier K^+ channel to which G_i/G_o–linked PTX-sensitive receptors commonly couple (18, 24).

Previously, in *Xenopus* oocytes mRNA-injected to express GIRK1 + GIRK4, a K^+ current was activated by ADP or 2-MeSADP through the co-expressed human $P2Y_{12}$ receptor (6), as predicted. We explored this further, using neuronal expression of the rat $P2Y_{12}$ receptor and another GIRK channel. The cDNAs of the rat GIRK1 and GIRK2 (Kir 3.1 and 3.2 subunits) and of EGFP (as marker of expressing cells), in mammalian expression vectors, were mixed and co-injected into the nuclei of the rat sympathetic neurons. A GIRK1/GIRK2 inward rectifier K^+ channels became expressed, as shown by the appearance of such a K^+ current induced by noradrenaline acting on endogeneous α_2-adrenoceptors (Fig.6A, upper panel). When the recombinant rat $P2Y_{12}$ receptor was co-expressed with the two GIRK subunits, those channels could also be activated by application of 2-MeSADP in the extracellular perfusion Krebs (6 mM K^+_o) solution (Fig. 6A, lower panel). 2-MeSADP strongly activated the channels even when only at 0.1 nM (Fig. 6A). Similar activation was also obtainable with 2-MeSATP (not shown). 2-MeSADP had no effect when the rat $P2Y_{12}$ plasmid was omitted or when (Fig.6A, upper panel) that plasmid was replaced by the same vector carrying

instead the EGFP cDNA. From concentration-response plots, exemplified in Fig. 6B, the coupling of the $P2Y_{12}$ receptor to the inward rectifier channel displayed an extremely high potency for 2-MeSADP (Table 2).

It was further found that in the P2Y family this activation of GIRK channels is not necessarily confined to a G_i/G_o-preferring receptor, as is the usual case in other receptor families (24, 25). The $G_{q/11}$-linked $P2Y_1$ receptor, when co-expressed instead of $P2Y_{12}$, produced with the same agonist (common to both subtypes) a similar fast activation of GIRK (Fig. 6D). However, with $P2Y_1$ this was followed by a slower but near-complete inactivation of the current while in the continued presence of the agonist. A similar secondary inactivation of P2Y-activated GIRK currents has been noted following stimulation of $P2Y_2$ receptors expressed in oocytes, and attributed to co-stimulation of phospholipase C and protein kinase C via G_q (26). In contrast, the current showed very little decline during prolonged agonist application in the neurons expressing $P2Y_{12}$ receptors (Fig.6 C, D).

The GIRK activation via the $P2Y_1$ receptor was abolished by PTX pre-treatment (not shown), paradoxically, the same behavior as that found with a range of G_i–linked G-protein-coupled receptors (GPCRs) in these neurons (18, 27). The reversal seen with $P2Y_1$ is not due to the agonist-induced internalization of GPCRs, since at the temperature of exposure and recording, ~20 ^oC, this should be absent, nor to classical desensitization since previously

(19) that was not seen with longer exposures of $P2Y_1$ receptors expressed in these cells to 2-MeSADP up to 10 μM concentration. Hence, the activated $P2Y_{12}$ receptor lacks a second type of reaction with GIRKs, which is produced by the $P2Y_1$ receptor, despite the essentially identical agonist profile (compare Table 1 with refs.17, 28) of these 2 receptors.

Coupling of the $P2Y_{12}$ receptor to voltage-gated Ca^{2+} and K^+ channels:

In experiments performed similarly with the $P2Y_{12}$ receptor but in the absence of GIRKs, 2-MeSADP inhibited the current through the endogenous N-type Ca^{2+} (Ca^{2+}_N) channel of the host neurons. At 1 μM 2-MeSADP, illustrating the maximum effect (Fig. 7A), the inhibition was 48.8 ± 4.3 % (n=14). This fraction of the population of these channels that is susceptible to $P2Y_{12}$ receptor-mediated inhibition is similar to that found for them with the other P2Y receptor subtypes studied (16, 17, 19). In control experiments (with neurons injected with the same vector carrying only the EGFP-cDNA) the inhibition of this Ca^{2+} current by 2-MeSADP or 2-MeSATP, up to 10 μM, was maximally 5.00 ± 2.04% (n = 9), the same non-significant change as was seen at 10 μM agonist with neurons not injected at all.

The potency of coupling of the $P2Y_{12}$ receptor to this Ca^{2+} channel was determined (Fig. 7B) and was also extremely high, about equal to that of coupling to the GIRK-channel (Table 2). 2-MeSATP was also shown to be an

agonist in this transduction, and with even higher potency than for 2-MeSADP (Fig. 7B; Table 2). This coupling was completely sensitive to pertussis toxin: when the toxin was absent, or present, in the incubation medium in the post-injection period (see Methods), the Ca^{2+} current was subsequently inhibited by 2-MeSATP (100 nM) by 49 ± 2% in the untreated cells (n=13) while in the parallel toxin-treated cells no inhibition was detectable.

The Ca^{2+}-current inhibition was accompanied by a marked slowing of the onset of the current (Fig. 7A), as we have observed for other P2Y receptors in the Ca^{2+} channel coupling. This suggests that the process is voltage-dependent (24, 27). This was confirmed, firstly by applying pre-pulses depolarizing to +90 mV; this strongly decreased the inhibitory action of 2-MeSATP (Fig. 8A,B). The extent of this effect matches the partial reduction found previously (19) with noradrenaline acting on the native adrenoceptors in these neurons under the same conditions. That effect was in other cases shown to be a voltage-dependent action due to released Gβγ-subunits inducing a gating shift of the channel (16, 27, 29). Further, the co-expression of the transducin Gα subunit, which sequesters free Gβγ subunits (24, 27), abolished the effect of the $P2Y_{12}$ receptor activation on the Ca^{2+} channel (Fig. 8A,B).

Effects on the M-current K^+ channel, which has been found previously (16, 19) to be blocked by the activation of other P2Y receptors, were also studied here. This current was unaffected by stimulation of the P2Y12 receptors expressed in these neurons (Table 2).

DISCUSSION

The B10 cell contains the identified $P2Y_{12}$ receptor

It is now clear that the inhibition of cAMP formation by adenine nucleotides in B10 rat brain capillary endothelial cells is due to an endogenous $P2Y_{12}$ receptor, identical to that in the platelet. Although initially in this study we had found that RT-PCR amplified a fragment corresponding to a stretch of the recently reported (6) $P2Y_{12}$ receptor sequence, this is not fully conclusive since it could be in a pseudogene or a non-translated mRNA: the cloning and heterologous expression of the $P2Y_{12}$ receptor from the B10 cells were necessary for absolute identification. The receptor cloned from those cells and expressed is shown to be functional, inhibiting stimulated adenylyl cyclase as in (3) the parent B10 cells. 2-MeSADP and 2-MeSATP are highly potent agonists in both cases (Table 1). However, there is a distinct strengthening of other agonists which were less potent in B10 cells (Table 1). The antagonist behavior of AR-C66096 and BzATP is also similar to that observed (3) for each in the B10 cell.

Agonists and antagonists of the $P2Y_{12}$ receptor in three situations

The agonist behavior of the adenosine triphosphates in the cAMP response of the expressed receptor from the B10 cell stands in contrast to their antagonist action in the platelet (as reviewed in the Introduction). Their agonism is seen here to be an intrinsic property of the $P2Y_{12}$ receptor. Further,

it exhibited that property also in another transduction and in a different host cell, the coupling to a neuronal Ca^{2+}-channel (Fig. 7). Hence, the possibility previously left open (3), that this difference is due to related but different P2Y subtypes in the B10 cell and in the platelet, can now be eliminated.

Further, that difference cannot arise from partial ecto-enzymic conversion of triphosphate to an agonistic diphosphate, as that was rigorously excluded here in all cases, and in any case the potency measured for 2-MeSATP clearly exceeded that of its putative product 2-MeSADP. Further, it is not affected by a species receptor variation (initially not completely excludable because the B10 cell is from rat and the platelet data on the triphosphates were all on the human platelet): the human $P2Y_{12}$ receptor, cloned from the platelet mRNA and expressed heterologously, also responds to adenosine triphosphates as agonists (Table 1). This difference with the triphosphates between the $P2Y_{12}$ receptor when in the platelet on the one hand and, on the other hand, in the B10 cell or when heterologously expressed in astrocytoma or CHO cells or sympathetic neurons, can be interpreted in terms of different receptor densities and receptor reserves in those states. Thus, the number of human $P2Y_{12}$ receptors at the CHO cell surface in an example of such a stable transfection was derived from the B_{max} of the specific binding of [^{33}P]2-MeSADP to the intact cells, as 477,000 ± 66,000 $P2Y_{12}$ receptors per cell (10). In comparison to this, from the B_{max} value of that binding reported for intact platelets and taking the clopidogrel-sensitive fraction thereof (10, 30,

31), we estimate after correcting for the relative surface areas of the two cell types that the mean number of $P2Y_{12}$ receptors per μm^2 of cell surface is of the order of 70-fold lower on the platelet..

Receptor theory, when formulated for modern concepts of GPCRs (32-34), still predicts that progressively raising receptor density from a low reserve will at first produce an increase in the maximal response of apparent partial agonists until they are full agonists, and at higher levels will increase the potency of all agonists. In some recent studies with other recombinant GPCRs where their expressed densities have been varied incrementally in the same host cell, this behavior has been verified for all agonists tested, while the potencies of competitive antagonists were unchanged, e.g. in refs (35, 36). In the present case, the diphosphate agonists for adenylyl cyclase inhibition in the human platelet indeed show lower potency there (8) than at the recombinant human $P2Y_{12}$ receptor. However, 2-MeSATP, ATP and 2-ClATP are changed from competitive antagonists in the platelet to agonists here. This effect cannot be ascribed to special conditions in an ectopic expression, since those three triphosphates similarly change to agonists at the native $P2Y_{12}$ receptor in B10 cells. In the B10 cell (3) they were of lower potency (9-68 fold) in decreasing the stimulated cAMP level than was found for them here in the heterologous expression of the same receptor, whereas the constant agonist 2-MeSADP had identical EC_{50} values in the two situations (Table 1). ATP and 2-ClATP were distinct partial agonists in B10 cells (3), while here they were as full agonists as 2-MeSADP (Figs. 2 and 8). All of these effects suggest a high

sensitivity of the $P2Y_{12}$ receptor to its density in the membrane.

However, an unusual case such as that of 2-MeSATP requires further explanation. The change there is extreme: it is the most potent agonist of those tested on the recombinant receptor (Table 1), but in the platelet it has long been known as a "P2T" receptor antagonist, and indeed behaves there as a strong competitive antagonist of ADP-induced adenylyl cyclase inhibition (K_B: 63 nM; ref. 14). In classical theory the action and potency of an antagonist has been considered to be independent of receptor reserve and, as noted above, this has been found in practice with GPCR antagonists when varying receptor expression level in several cases in recent years. However, the current availability of many of the GPCRs in constitutively active form has shown that the majority of ligands known as antagonists are in reality agonists of negative or low positive efficacy (34, 37), which appear as antagonists when they compete well in binding with more efficacious agonists. Although it must be kept in mind that efficacy in a GPCR is a highly complex quantity, the resultant of a presently unknown set of microscopic equilibrium constants of receptor reactions, as emphasized by Colquhoun (38), efficacy will then, when used in empirical comparisons, still be subject to mass-action effects of the receptor concentration in those equilibria. Reactions of apparent antagonists as just defined will, as for all other agonists, have the potential to show the earlier described effects of raising the receptor concentration. Since they start from a very low efficacy such ligands, in particular, can have the potential for such effects to be large. Those effects will not be seen with a true antagonist, i.e. a

ligand that binds at the site with no productive conformational change. It appears that 2-MeSATP is an apparent antagonist at low receptor density, as in the platelet. It can therefore be shifted at to a higher (empirical) efficacy at the (presumed) moderate receptor density in the B10 cell and further at high density (in recombinant expression) to very high agonist potency. ATP and 2-ClATP appear to be in the same category, but with weaker interactions with the $P2Y_{12}$ receptor. On the other hand, true antagonist behavior can also exist in the present system, as in the halogenated ATP derivative AR-C66096, which remains a competitive antagonist of similar potency at all densities of the $P2Y_{12}$ receptor, in the platelet (39), the B10 cell (3) and here (Fig. 3). Support for this interpretation is given, firstly by unexpected effects of receptor density on the activity of some other GPCRs, as reviewed by Kenakin (40). A striking parallel to the present case can be found with the $5HT_{1A}$ receptor. There, Hoyer and Boddeke (41) report the conversion of four strong competitive antagonists (pK_B values as high as 8.2) to highly potent agonists, by an increase in the receptor level of 7-fold. In this and some similar cases cited there, the comparisons were made on a receptor stably expressed at different, measured densities in a given host cell line and transduction. This shows that this density effect is not due to differing effector environments, as, e.g., here between the platelet and the B10 cell. Secondly, a similar set of changes from antagonist to agonist behavior in different expression situations also has been documented with another P2Y subtype, $P2Y_1$, and found to hold for different transductions which it mediates (17, 28, 42, 43). An additional

effect of higher density could operate if these receptors can form homo-dimers, for which there is recent evidence with some GPCRs, which could lead to efficacy and affinity increases occurring with higher receptor concentration (44). Homo-dimer formation has not been examined for P2Y receptors.

Occurrence of the $P2Y_{12}$ receptor outside the platelet

While much is known on the function in the platelet (12, 14, 39, 45, 46) of a long-known (13) adenylyl cyclase-inhibitory receptor there now isolated as the $P2Y_{12}$ receptor, it is interesting to see that the same receptor exists in other cell types. As well as being cloned here from brain microvascular endothelial cells, a similar activity was detected in the C6 glioma cell line or its derivative C6-2B (47-49).

That cyclase-inhibitory ADP receptor has been studied with purified nucleotides and demonstrates agonist activities very similar to those found likewise with B10 cells, including, again, agonist activity for the adenosine triphosphates (8). Jin *et* al. (50) have found evidence from PCR indicating that the C6-2B glioma cell expresses the $P2Y_{12}$ receptor. In Northern blots of human tissue extracts, Hollopeter *et al.* (6) found $P2Y_{12}$ mRNA in platelets and brain only. Zhang *et al.* (7) also found it strongly in platelets and in all brain regions (plus spinal cord) tested, weakly in lung, pituitary and adrenal gland, but not in many other tissues tested. *In situ* hybridization of mRNA in brain sections showed reaction throughout white and gray matter, consistent with glial expression (6). Microglia could contribute to the expression seen, since

Honda *et al.* (51) report that chemotaxis in brain microglia in culture is increased by ATP, with pharmacology that corresponds to the $P2Y_{12}$ receptor. If the brain microvasculature expresses the $P2Y_{12}$ receptor sufficiently, that site would also contribute to the *in situ* distribution observed. In those endothelial cells its function is at present unknown but they are intimately associated in the blood-brain barrier with astrocytes, while $[Ca^{2+}]_i$ increase and cAMP levels are important in the barrier permeability control (52). A local source of ATP (and hence ADP) would be from the astrocytes, which are known (53) to secrete it, or from the endothelium itself.

Coupling of the $P2Y_{12}$ receptor to G-proteins and ion channels

The coupling of the $P2Y_{12}$ receptor to closure of a voltage-gated Ca^{2+} channel, here shown for the N-type channel, is a new aspect of its transduction. The Ca^{2+}_N channels are characteristic of neurons; the very limited evidence available on $P2Y_{12}$ receptors in the CNS, noted above, as yet does not exclude that some neurons contain it, along with some non-neuronal CNS sites. However, the ability has not yet been tested of activated $P2Y_{12}$ receptors to block also L-type voltage-gated Ca^{2+} channels in non-neuronal cells; such dual actions on Ca^{2+}_N and Ca^{2+}_L channels, both PTX-sensitive, are known with another G_i /G_o -specific receptor, mGlu2 (54).

The B10 cell contains $G\alpha_o$ and all three $G\alpha_i$ subunits (Fig. 5A), as do the astrocytoma host cells used (Fig. 5B). Our findings on the couplings to both a Ca^{2+} and an inward rectifier K^+ channel provide evidence on some functional G-protein interactions of the $P2Y_{12}$ receptor. Both actions can be ascribed to release of a $G\beta\gamma$ subunit pair from the heterotrimeric-G-protein/$P2Y_{12}$ complex and its direct action on the K^+ or Ca^{2+} channel. The activation of GIRK in all other cases studied has been established to be mediated thus (18, 24), generally from a PTX-sensitive G-protein (as here); where a native G-protein was identified, this is from the G_i and not the G_o sub-class (e.g. refs. 18, 25). (Other such cases where the $G\alpha$ subtypes involved were compared using heterologous expression of those showed some apparent promiscuity). GPCR-mediated block of a Ca^{2+} channel is likewise known to be via released $G\beta\gamma$ subunits (24, 27, 29, 55) and this was confirmed to hold for the $P2Y_{12}$ receptor (Fig. 8). For $P2Y_{12}$, that action at the Ca^{2+}_N channel was also completely PTX-sensitive; in such voltage-dependent inhibition at the Ca^{2+}_N channel coupled to a variety of native receptors in neurons, so far only heterotrimers of $G\alpha_o$ and $G\alpha_{i2}$, but not $G\alpha_{i1}$ or $G\alpha_{i3}$,have been found to act (29, 56). In support of that case here, the ADP-induced inhibition of adenylyl cyclase in the platelet (now known to be by the $P2Y_{12}$ receptor) was impaired (57) in mice in which the $G\alpha_{i2}$ gene has been disrupted.

The G-protein subunit involved in GPCR-mediated closing the M-current K^+ channel in SCG neurons has been shown to be α_q (58). P2Y receptors, which activate phospholipase C via $G_{q/11}$ readily give, where tested, this M-current inhibition, but unusually, also the Ca^{2+}_N channel closure (16,17,19, 23). The $P2Y_{12}$ receptor, alone in that family so far, shows the latter coupling but none of the former. Thus, the dual $G\alpha$ specificity of the others when expressed in the SCG neuron does not arise with $P2Y_{12}$. That difference is also illustrated by the ability of the $P2Y_1$ receptor to give additionally the G_i-type GIRK activation and a subsequent inactivation in the presence of agonist involving some other, as yet unidentified, G-protein, whereas $P2Y_{12}$ produces only the pure G_i-type response (Fig. 6C,D).

The potency of the agonist tested for these actions, 2-MeSADP, is an order of magnitude greater than for the adenylyl cyclase inhibition (Tables 1 and 2). This exceptional strength is not attributable to an artificially high concentration of the effector channels created by the micro-injection of GIRK subunits, since it is found equally with the native N-type Ca^{2+} channels of the host neuron. The $G\beta\gamma$ interaction with inward rectifier K^+ and voltage-gated Ca^{2+} channels are primary, rapid transduction steps independent of second messengers and downstream (43, 59) P2Y signaling. The release of $G\beta\gamma$ subunits appears to be particularly effective with the $P2Y_{12}$ receptor.

ACKNOWLEDGEMENTS

This work was supported in part by grants from the Wellcome Trust to EAB and DAB and from the Research Grants Council of Hong Kong (2/99C) to YHW. We thank Dr. F. Lesage (CNRS, Sophia Antipolis) for the GIRK1 and GIRK2 plasmids.

REFERENCES

1. Feolde, E., Vigne, P., Breittmayer, J-P. and Frelin, C. (1995) *Br. J. Pharmacol.* **115,** 1199-1203
2. Webb, T.E., Feolde, E., Vigne, P., Neary, J.T., Runberg, A., Frelin, C. and Barnard, E.A. (1996) *Br. J. Pharmacol.* **119,** 1385-1392
3. Simon, J., Vigne, P., Eklund, K.M., Michel, A.D., Carruthers, A.M., Humphrey, P.P.A., Frelin, C. and Barnard, E.A. (2001) *Br. J. Pharmacol.* **132,** 173-182
4. Humphries, R.G., Tomlinson, W., Ingall, A.H., Cage, P.A. and Leff, P. (1994) *Br. J. Pharmacol.* **113,** 1057-1063
5. Jin, J., Daniel, J.L. and Kunapuli, S.P. (1998) *J. Biol. Chem.* **273,** 2030-2034
6. Hollopeter, G., Jantzen, H-M., Vincent, D., Li, G., England, L., Ramakrishnan, V., Yang, R-B., Nurden, P., Nurden, A., Julius, D. and Conley, P. (2001) *Nature*, **409,** 202-207
7. Zhang, F.L., Luo, L., Gustafson, E., Lachowicz, J., Smith, M., Qiao, X., Liu, Y-H., Chen, G., Pramanik, B., Laz, T.M., Palmer, K., Bayne, M. and Monsma, F. (2001) *J. Biol. Chem.* **276,** 8608-8615
8. Barnard, E.A. and Simon, J. (2001) *Trends Pharmacol. Sci.* **22,** 388-391
9. Takasaki, J., Kamohara, M., Saito, T., Matsumoto, M., Matsumoto, S-I., Ohishi, T., Soga, T., Matusushime, H. and Furuichi, K. (2001). *Mol.*

Pharmacol. **60,** 432-439

10. Savi, P., Labouret, C., Delesque, N., Guette, F., Lupker, J. and Herbert, J.M. (2001) *Biochem. Biophys. Res. Commun.* **283,** 379-383
11. Hourani, S.M. and Hall, D.A. (1994) *Trends Pharmacol. Sci.*, **15,** 103-108
12. Kunapuli, S.P. (1998) *Trends Pharmacol. Sci.* **19,** 392-394
13. Cusack, N.J. and Hourani, S.M.O. (1982) *Br. J. Pharmacol.* **77,** 329-333
14. Park, H.S. and Hourani, S.M.O. (1999) *Br. J. Pharmacol.* **127,** 1359-1366
15. Carruthers, A.M., Warner, A.J., Michel, A.D., Feniuk, W. and Humphrey, P.P.A. (1999) *Br. J. Pharmacol.* **126,** 1221-1229
16. Filippov, A.K., Webb, T.E., Barnard, E.A. and Brown, D.A. (1998) *J. Neurosci.* **18,** 5170-5179
17. Filippov, A.K., Brown, D.A. and Barnard, E.A. (2000) *Br. J. Pharmacol.* **129,** 1063-1066
18. Fernandez-Fernandez, J.M., Abogadie, F.C., Milligan, G., Delmas, P. and Brown, D.A. (2001) *Eur. J. Neurosci.* **14**, 283-292
19. Filippov, A.K., Webb, T.E., Barnard, E.A. and Brown, D.A. (1999) *Br. J. Pharmacol.* **126,** 1009-1017
20. King, B.F. and Townsend-Nicolson, A. (2000) *J. Autonom. Nerv. System.* 81, 164-170
21. Wong, Y.H., Conklin, B.R. and Bourne, H.R. (1992) *Science* **255,** 339-342
22. Lounsbury, K.M., Casey, P.J., Brass, L.F. and Manning, D.R. (1991) *J.*

Biol. Chem. **266,** 22051-22056

23. Brown, D.A., Filippov, A.K. and Barnard, E.A. (2000) *J. Autonom. Nerv. System.* **81,** 31-36
24. Clapham, D.E. and Neer, E.J. (1997) *Annu. Rev. Pharmacol. Toxicol.* **37,** 167-203
25. Lledo, P.M., Homburger, V., Bockaert, J. and Vincent, J.D. (2000) *Neuron* **8,** 455-463
26. Mark, M.D., Ruppersberg, J.P. and Herlitze, S. (2000) *Neuropharmacology* **39,** 2360-2373
27. Dolphin, A.C.(1998) *J. Physiol.* **506,** 3-11
28. Palmer, R.K., Boyer, J.L., Schachter, J.B., Nicholas, R.A. and Harden, T.K. (1998) *Mol. Pharmacol.* **54,** 1118-1123
29. Delmas, P., Abogadie, F.C., Milligan, G., Buckley, N.J. and Brown, D.A. (1999) *J. Physiol.* **518**, 23-36
30. Savi, P., Beauverger, P., Labouret, C., Delfaud, J., Picard, C., Maffrand, J.P., Pascal, M. Herbert, J.M. (1998) *FEBS Lett.* **422,** 291-295
31. Hechler, B., Eckly, A., Ohlmann, P., Cazenave, J.P. and Gachet, C. (1998) *Br. J. Haematol.* **103**, 858-866
32. Black, J.W. and Leff, P. (1983) *Proc. R. Soc. Lond. B. Biol. Sci.* **220,** 141-162
33. Kenakin, T.P. (1997) Pharmacological analysis of drug-receptor interaction. *3rd Edition. Lippincott-Raven, New York.*
34. Kenakin, T.P. (1999) *Trends Pharmacol. Sci.,* **20***,* 400-405
35. Zhong, H., Guerrero, S.W., Esbenshade, T.A. and Minneman, K.P.

(1996) *Mol. Pharmacol.* **50**, 175-184.

36. Hermans, E., Challis, R.A.J. and Nahorski, S.R. (1999) *Br. J. Pharmacol.,* **126**, 873-882.

37. Milligan, G. and Bond, R.A. (1997) *Trends Pharmacol. Sci.* **17,** 468-474

38. Colquhoun, D. (1998) *Br. J. Pharmacol.* **125,** 924-947

39. Daniel, J.L., Dangelmayer, C., Jin, J., Ashby, B., Smith, J.B. and Kunapuli, S.P. (1998) *J. Biol. Chem.* **273,** 2024-2029

40. Kenakin, T.P. (1996) *Pharmacol. Rev.* **48***,* 413-463

41. Hoyer, D. and Boddeke, H.W. (1993) *Trends Pharmacol. Sci.*, **14,** 270-275

42. Hechler, B., Vigne, P., Leon, C., Breittmayer, J-P., Gachet, C. and Frelin, C. (1998). *Mol. Pharmacol.* **53,** 727-733

43. Sellers, L.A., Simon, J., Lundahl, T.S., Cousens, D.J., Humphrey, P.P.A. and Barnard, E.A. (2001) *J. Biol. Chem.* **276,** 16379-16390

44. Onaram, H.O. and Gürdal, H. (1999) *Trends Pharmacol. Sci.* **20,** 274-278

45. Jantzen, H-M., Gousset, L., Bhaskar, V., Vincent, D., Tai, A., Reynolds, E.E. and Conley, P.B. (1999) *Thromb. Haemost.* **81,** 111-117

46. Leon, C., Hechler, B., Freund, M., Eckly, A., Vial, C., Ohlmann, P., Dierich, A., Lemeur, M., Cazenave, J-P. and Gachet, C. (1999) *J. Clin. Invest.* **104,** 1731-1737

47. Pianet, I., Merle, M. and Labouesse, J. (1989) *Biochem. Biophys. Res. Commun.* **163,** 1150-1157

48. **Valeins**, H., Merle, M., and Labouesse, J. (1992) *Mol. Pharmacol.* **42**, 1033-1041

49. Boyer, J.L., Lazarowski, E.R., Chen, X-H. and Harden, T.K. (1993) *J. Pharmacol. Exp. .Ther.* **267,** 1140-1146

50. Jin, J., Tomlinson, W., Kirk, I.P., Kim, Y.B., Humphries, R.G. and Kunapuli, S.P. (2001) *Br. J. Pharmacol.* **133,** 521-528

51. Honda, S., Sasaki, Y., Ohsawa, K., Imai, Y., Nakamura, Y., Inoue, K. and Kohsaka, S. (2001) *J. Neurosci.* **21,** 1975-1982

52. Abbott, N.J. and Revest, P.A. (1991) *Cerebrovasc. Brain Metab. Rev.* **31,** 1-34

53. Anwar, Z., Albert, J.L., Gubby, S.E., Boyle, J.P., Roberts, J.A., Webb, T.E. and Boarder, M.R. (1999) *Br. J. Pharmacol.* **128,** 465-471

54. Perroy,J., Gutierrez, G.J, Coulon, V., Bockaert. J., Pin, J.P. and Fagni, L. (2001) *J. Biol. Chem.* **276,** 45800-45805

55. Lei, O., Jones, M.B., Tallet, E.M., Schrier, A.D., McIntire, W.E., Garrison, J.C. and Bayliss, D.A. (2000) *Proc. Natl. Acad. Sci. USA*, **97,** 9771-9776

56. Jeong, S.W. and Ikeda, S.R. (2000) *Proc. Natl. Acad. Sci. USA*, **97,** 907-912

57. Jantzen, H-M., Milstone, D.S., Gousset, L., Conley, P.B. and Mortensen R.M. (2001) *J. Clin. Invest.* **108,** 477-483

58. Haley, J.E., Abogadie, F.C., Delmas, P., Dayrell, M., Vallis, Y., Milligan, G., Caulfield, M.P., Brown, D.A. and Buckley, N.J. (1998) *J. Neurosci.* **18**, 4521-4531

59. Claes, P., Grobben, B., Van, Kolen, K., Roymans, D. and Slegers, H. (2001) *Br. J. Pharmacol.* **134,** 402-408

FOOTNOTES

[1]The abbreviations used are: A3P5P, adenosine-3'-phosphate-5'-phosphate; A2P5P, adenosine-2'-phosphate-5'-phosphate; AR-C66096, 2-propylthio-D-β,γdifluoromethyleneATP; 2-MeSADP, 2-methylthioADP; 2-MeSATP, 2-methylthioATP; ADP²S, adenosine 5-*O*-(2-thio)diphosphate; 2-ClATP, 2-chloroATP; BzATP, 2&3-*O*-(4-benzoylbenzoyl)-adenosine 5-triphosphate; Ca^{2+}_N, N-type Ca^{2+} channel; GIRK, G-protein-coupled inward rectifier K^+-channel; cAMP, cyclic-AMP; IBMX, 3-isobutyl-1-methylxanthine; PKA, protein kinase A; CHO, Chinese Hampster Ovary; RT-PCR, Reverse Transcriptase-Polymerase Chain Reaction; DMEM, Dulbecco's Modified Eagle's Medium; FBS, fetal bovine serum; PTX, pertussis toxin; PMSF phenylmethylsulfonyl fluoride; DTT, dithiothreitol; PBS, phosphate-buffered saline; EGFP, enhanced Green Fluorescent Protein; GPRC, G-protein-coupled receptor.

LEGENDS TO FIGURES

Fig. 1. Alignment of the deduced amino acid sequence of the rat (B10 cell) and the human $P2Y_{12}$ receptors. The *overlined* amino acid sequences are the transmembrane domains (TMs) predicted from hydropathy profiles and alignment with other P2Y sequences. For the human $P2Y_{12}$ receptor the differences in the amino acid sequence are shown.

Fig. 2. Concentration-dependent effects of agonists at the rat $P2Y_{12}$ receptor stably expressed in 1321N1 astrocytoma cells. The percentage inhibition of the forskolin-stimulated cAMP accumulation (see Methods) is shown. Data are represented as the mean ± s.e.mean from 6-19 independent determinations (each performed in triplicate) for each agonist, and are fitted to a logistic equation.

Fig. 3. Concentration-dependent antagonism of the 2-MeSADP-mediated inhibition of the forskolin-stimulated cAMP formation in 1321N1 cells, stably expressing the rat $P2Y_{12}$ receptor (data obtained and plotted as for Fig. 2). The selective $P2Y_T$ antagonists AR-C66096 (**A**) or BzATP (**B**) are used. cAMP accumulation in the presence of 10 μM forskolin but in the absence of agonist and antagonist was taken as 100 %. From the computed EC_{50} values for each curve, Schild plots were constructed (not

shown) and K_B values for each antagonist were calculated (Table 1).

Fig. 4. Pertussis toxin 2-MeSADP-induced inhibition of forskolin-stimulated cAMP formation in 1321N1 cells, heterologously expressing the rat $P2Y_{12}$ receptor. The cells were either treated with 100 ng/ml pertussis toxin (upper plot) or with culture medium (lower plot) for 16 h at 37°C (see Methods for details).

Fig. 5. Relevant G-protein subunits present in B10 (A) and 1321N1 (B) cells. Protein extracts of the cell membranes were analyzed in Western blots. The blots were probed with antisera specific for each of the G-protein subunits indicated. Electrophoretic mobilities of marker proteins are also shown.

Fig. 6. Modulation of an inward rectifier channel by activation of the rat $P2Y_{12}$ or $P2Y_1$ receptors. The neurons were co-injected intranuclearly, one day prior to recording, with 3 plasmids, expressing GIRK1, GIRK2 (100 ng/µl each) and (as a marker of expression) EGFP (25 ng/µl). Where shown, a fourth plasmid expressing a P2Y receptor was added (100 ng/µl) with these. **A,** GIRK currents were evoked by 200-ms ramps between –140mV and –40 mV from a holding potential of –60 mV in perforated patch mode (16) and returned to the holding potential. Upper records: expression of the inward rectifier channel is shown by the responses recorded before (Control) and

after application of noradrenaline to activate the endogenous α_2-adrenoceptor. For confirmation, when immediately followed by application of 1 mM Ba^{2+} the GIRK-current was completely blocked. Lower records: when the $P2Y_{12}$ receptor was co-expressed, 2-MeSADP activated the GIRK current (again Ba^{2+}-sensitive), acting at very low concentrations (response at 0.1 nM is shown). In contrast, without the nucleotide receptor expressed 2-MeSADP was ineffective even at 1 μM (upper records; curve superimposes with the agonist-free control curve). **B,** concentration dependence of the GIRK-current activation by 2-MeSADP in $P2Y_{12}$ -expressing cells. Currents were measured at 20 ms after ramp start. Activated currents were measured as the current after agonist application less the current before agonist application and normalized for each cell to its maximally-activated current. Points show means $\pm$ s.e.mean of replicate measurements on 3-5 cells; concentrations were added cumulatively. Theoretical curves were fitted to the pooled data points by the Hill equation (see Methods). **C** and **D**, for co-injected neurons expressing $P2Y_{12}$ (C) or $P2Y_1$ (D) receptors, plots of the GIRK current as measured every 5 seconds at 20 ms after each ramp start. Note that stimulation of $P2Y_{12}$ receptors produced a near-stable activation of the GIRK current, whereas $P2Y_1$ stimulation produced a transient activation of the GIRK current followed by inactivation.

Fig. 7. Modulation of the N-type Ca^{2+}-channel by activation of the $P2Y_{12}$ receptor. The neurons were pre-injected with plasmids containing the rat $P2Y_{12}$ receptor cDNA (100 ng/μl) and the EGFP cDNA (25 ng/μl) as before. Currents through N-type Ca^{2+} channels were elicited by voltage steps and recorded as described in Methods. **A,** the superimposed leak-subtracted currents in the absence and presence of 2-MeSADP, 1 μM. Note that 2-MeSADP both decreased the current and dramatically slowed the kinetics of its activation. **B,** concentration dependence of the Ca^{2+} channel current inhibition by 2-MeSADP or 2-MeSATP. The % decrease was measured 10 ms from the onset of the test pulse: plots were obtained as for Fig.6.

Fig. 8. G-protein βγ-subunits are responsible for $P2Y_{12}$ receptor mediated inhibition of the Ca^{2+} channel current. A, records showing super-imposed $I_{Ca(N)}$ obtained with a double-pulse voltage protocol (as marked at the top) in the absence (control) and presence of 100 nM 2-MeSATP. The cells were pre-injected with the $P2Y_{12}$-cDNA-containing plasmid as before, alone (upper records) or together with a transducin-Gα- cDNA-containing plasmid (200 ng/μl , lower records). **B**, bar-charts showing the mean % current inhibition (measured after 10 ms at 0 mV command potential) produced by 2-MeSATP before (Prep0) and after (Prep90) the +90 mV prepulse in *n* cells injected with $P2Y_{12}$ cDNA alone

(first 2 bars) or together with transducin-Gα cDNA (last 2 bars). *, the inhibition is significantly decreased by the +90mV prepulse, p= 0.0045: this, and also its elimination of the slowing of the kinetics as seen in panel A, demonstrate voltage-dependence of the $P2Y_{12}$ -mediated effect. **, with or without a prepulse, the inhibition by 2-MeSATP is abolished when transducin-Gα is expressed ($p< 0.001$ for comparison of Prep0 bars without and with transducin-Gα ; the last 2 bars are not significantly different, at $p=0.24$).

TABLE 1.

Agonist and antagonist potencies of heterologously expressed $P2Y_{12}$ receptors in inhibition of cAMP accumulation.

The EC_{50} values of agonists were determined from logistic fitting of the data as in Fig. 2, and the K_B values for antagonists were obtained from Schild plots generated from data fitted as in Fig. 4. Values (mean ± s.e.m) presented were obtained here from 3 -19 independent determinations (n.d., not determined) or are quoted from references (3, 7).

Agent	Rat receptor				Human receptor[c]	
	Recombinant[a]		Native in B10 cells[b]			
	Agonist	Antagonist	Agonist	Antagonist	Agonist	
	EC_{50} (nM)					
	EC_{50} (nM)	K_B (nM)	EC_{50} (nM)	K_B (nM)		
A	B (ref. 7)					
2-MeSADP	2.0±0.2	2.2	2.1±0.4	14±2		
2-MeSATP	0.4±0.04	3.5	0.24±0.03	3±0.5		
ADP	75±10	3100	61±16	61±10		
ADPβS	103±31	623	n.d.	191±20		
ATP	1,868±293	26,000[d]	1,250±180	n.d.		
2-ClATP	194±9	13,500[d]	95±10	636±100		
AR-C66096	28±5	39				

BzATP	9,030±300	2,100

[a]The rat $P2Y_{12}$ receptor cloned from B10 cells and heterologously expressed in 1321N1 cells (this work) or [b]endogeneously expressed in rat B10 cells (3). [c]The human $P2Y_{12}$ receptor: (A) cloned from genomic DNA and heterologously expressed in CHO-K1 cells (this work); (B) heterologously expressed in CHO-$DHFR^-$ cells (7). [d]These were partial agonists (3), efficacy ~0.5. For all other cases shown for the rat receptor the agonist did not differ significantly from full efficacy.

TABLE 2

Hill equation parameters for agonist-mediated actions of the rat P2Y$_{12}$ receptor on ion channels in injected neurons

Pooled data points were used to obtain Hill equation parameters as detailed in Methods. Each value is the mean ± s.e.mean.

Channel	Agonist	EC_{50} (nM)	n_H
GIRK1/2 [a]	2-MeSADP	0.099 ± 0.008	0.99 ± 0.07
N-type Ca^{2+}-channel [b]	2-MeSADP	0.107 ± 0.022	0.76 ± 0.11
N-type Ca^{2+}-channel [b]	2-MeSATP	0.042 ± 0.007	0.87± 0.12
M-current K^+-channel	2-MeSADP	No action [c]	

[a]Activation; values derived from plots as in Fig.6. [b]Inhibition; values derived from plots as in Fig. 7. [c]No detectable action on M-current at 2-MeSADP concentrations up to 1000 nM (n= 4 neurons). In the same neurones, the muscarinic agonist oxotremorine-M (10 μM) inhibited M-current by 74.2 ± 4.8% as previously (14). Also in all neurones tested from the same batch, 2-MeSADP produced normal inhibition of the Ca^{2+} channel current,

indicating that the $P2Y_{12}$ receptor was fully expressed.

Simon *et al.*, Fig. 1

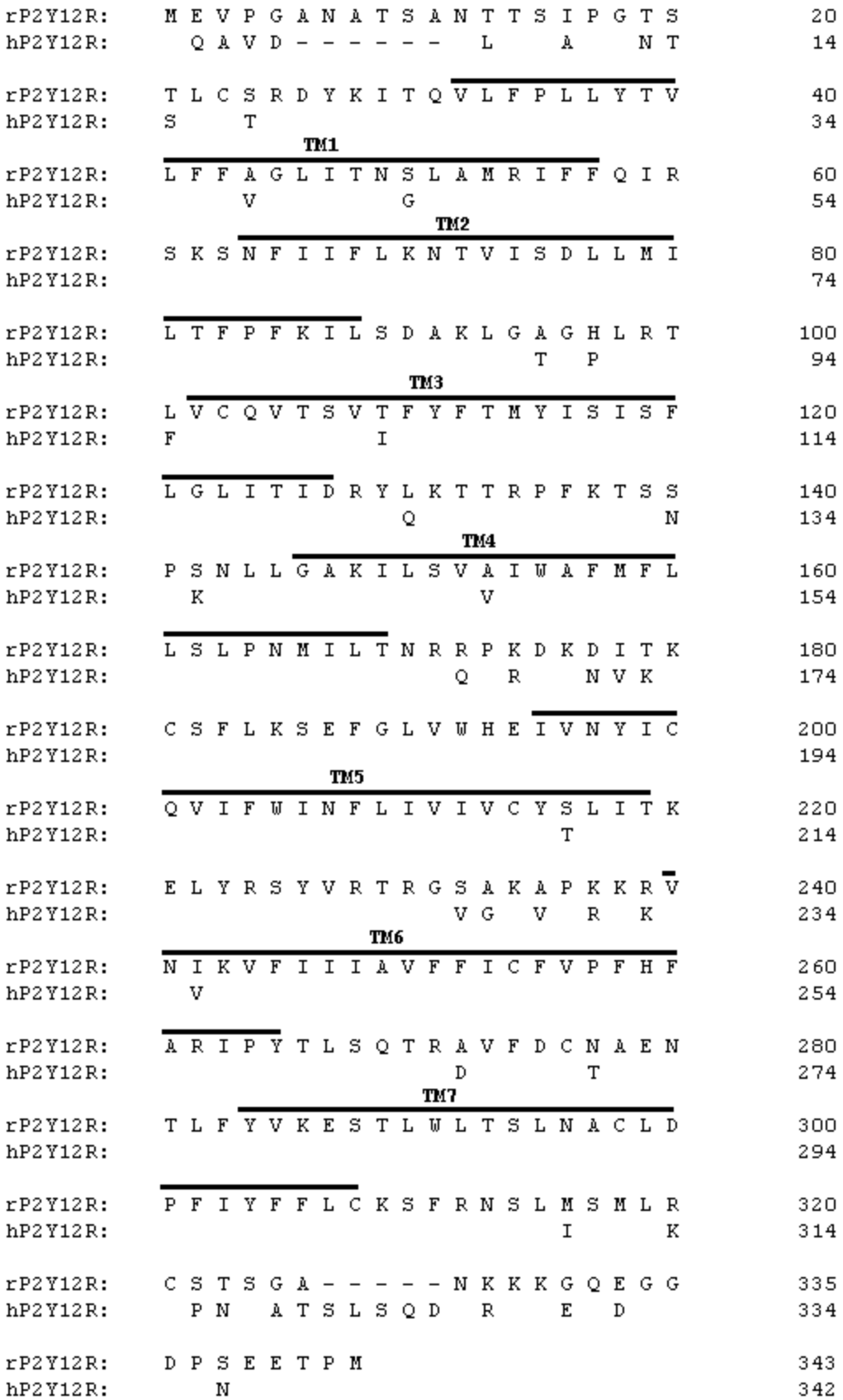

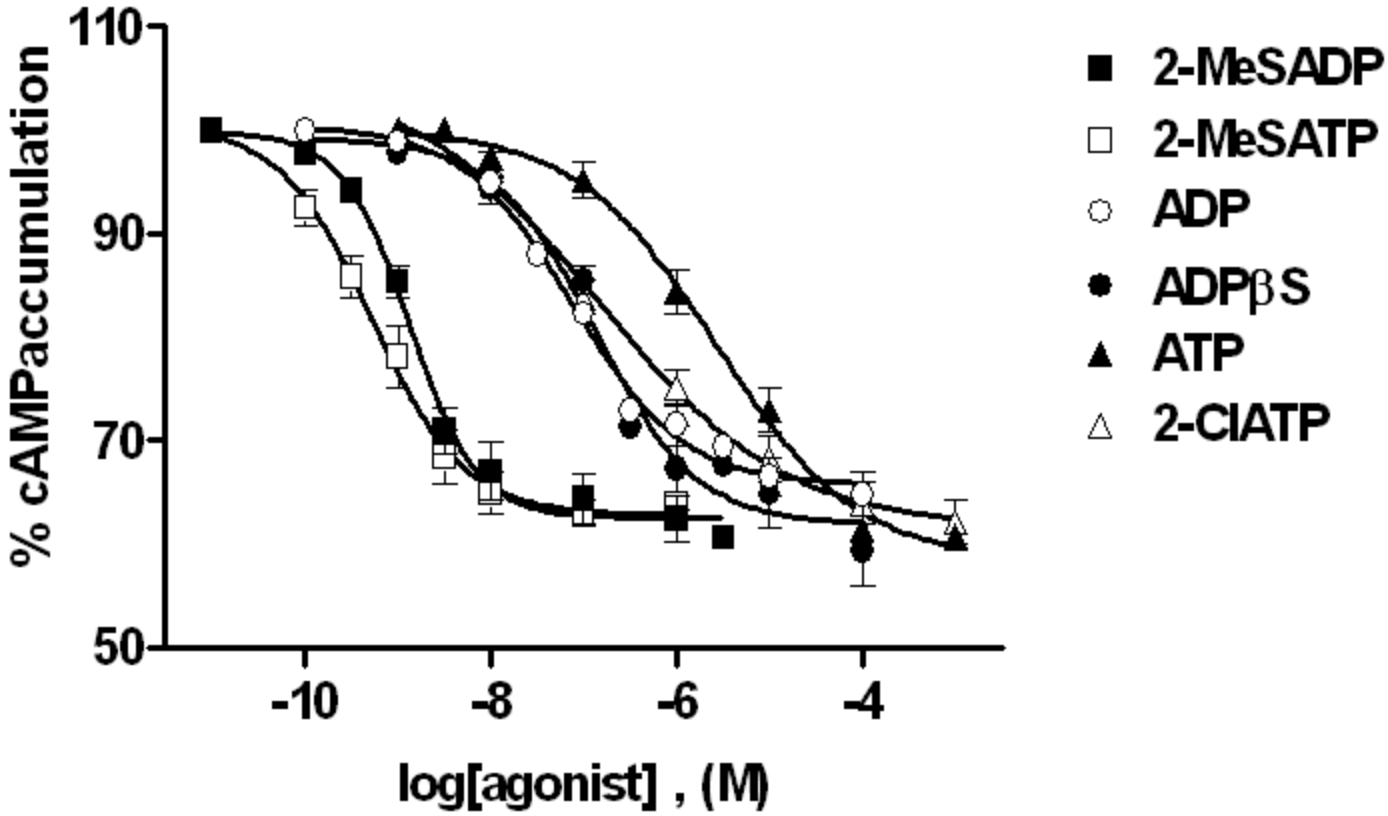
110
90
70
50
% cAMPaccumulation
-10
-8
-6
-4
log[agonist] , (M)
2-MeSADP
2-MeSATP
ADP
ADPβS
ATP
2-ClATP

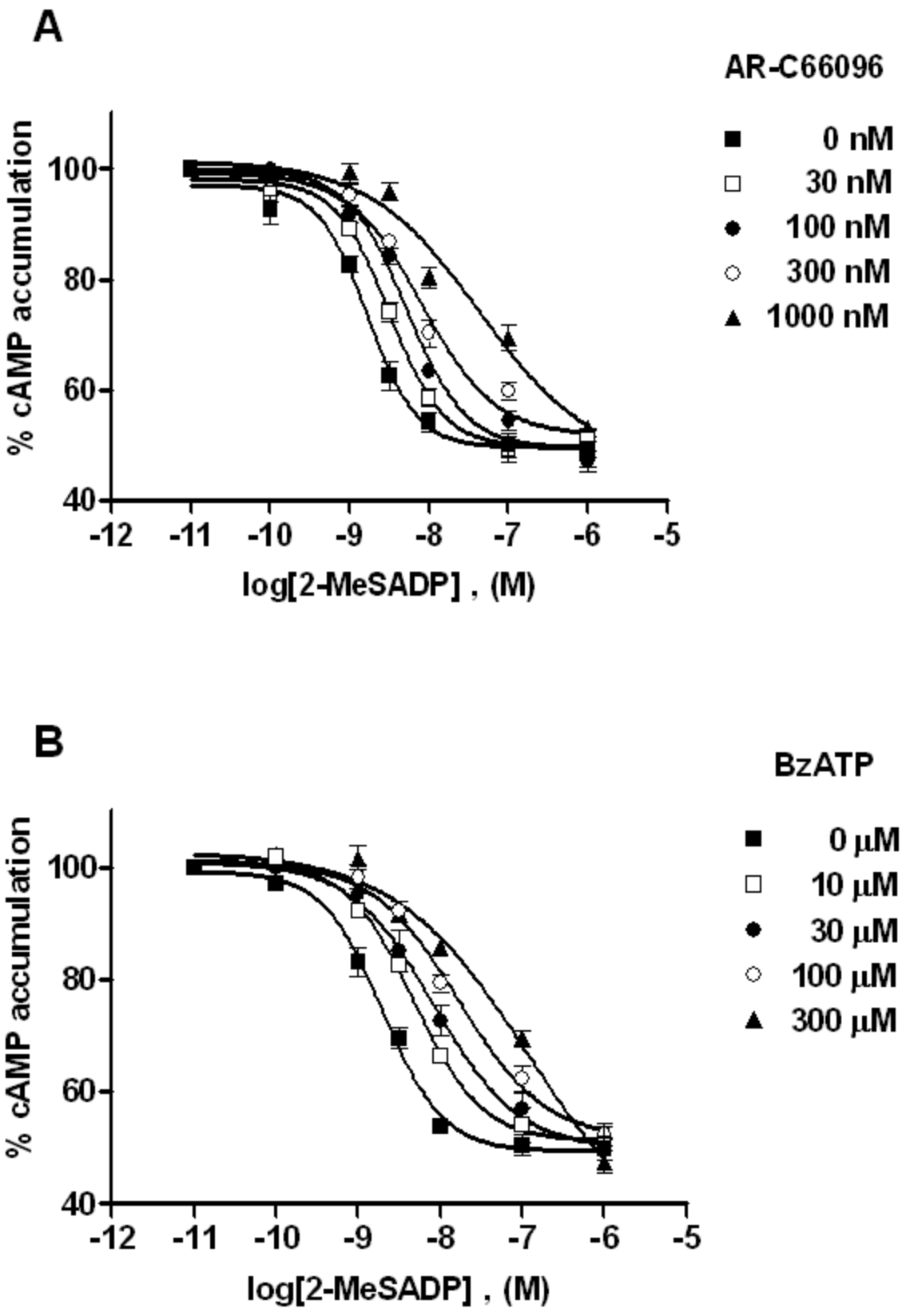
A
AR-C66096
0 nM
30 nM
100 nM
300 nM
1000 nM
% cAMP accumulation
100
80
60
40
-12
-11
-10
-9
-8
-7
-6
-5
log[2-MeSADP] , (M)
B
BzATP
0 μM
10 μM
30 μM
100 μM
300 μM
% cAMP accumulation
100
80
60
40
-12
-11
-10
-9
-8
-7
-6
-5
log[2-MeSADP] , (M)

Simon *et al.*, Fig. 4

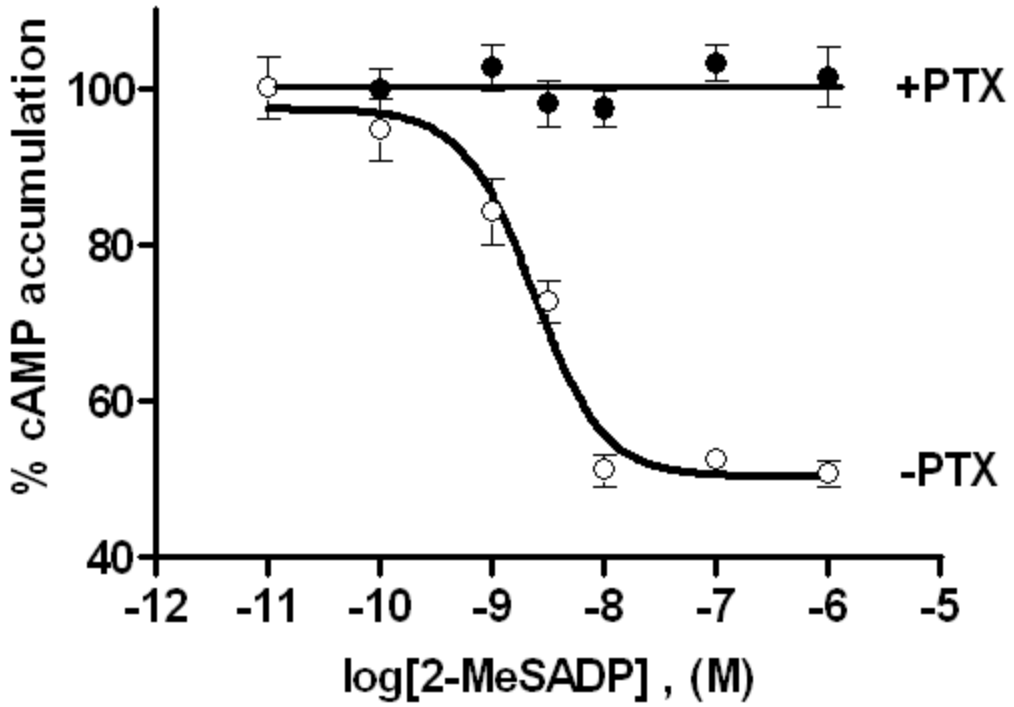

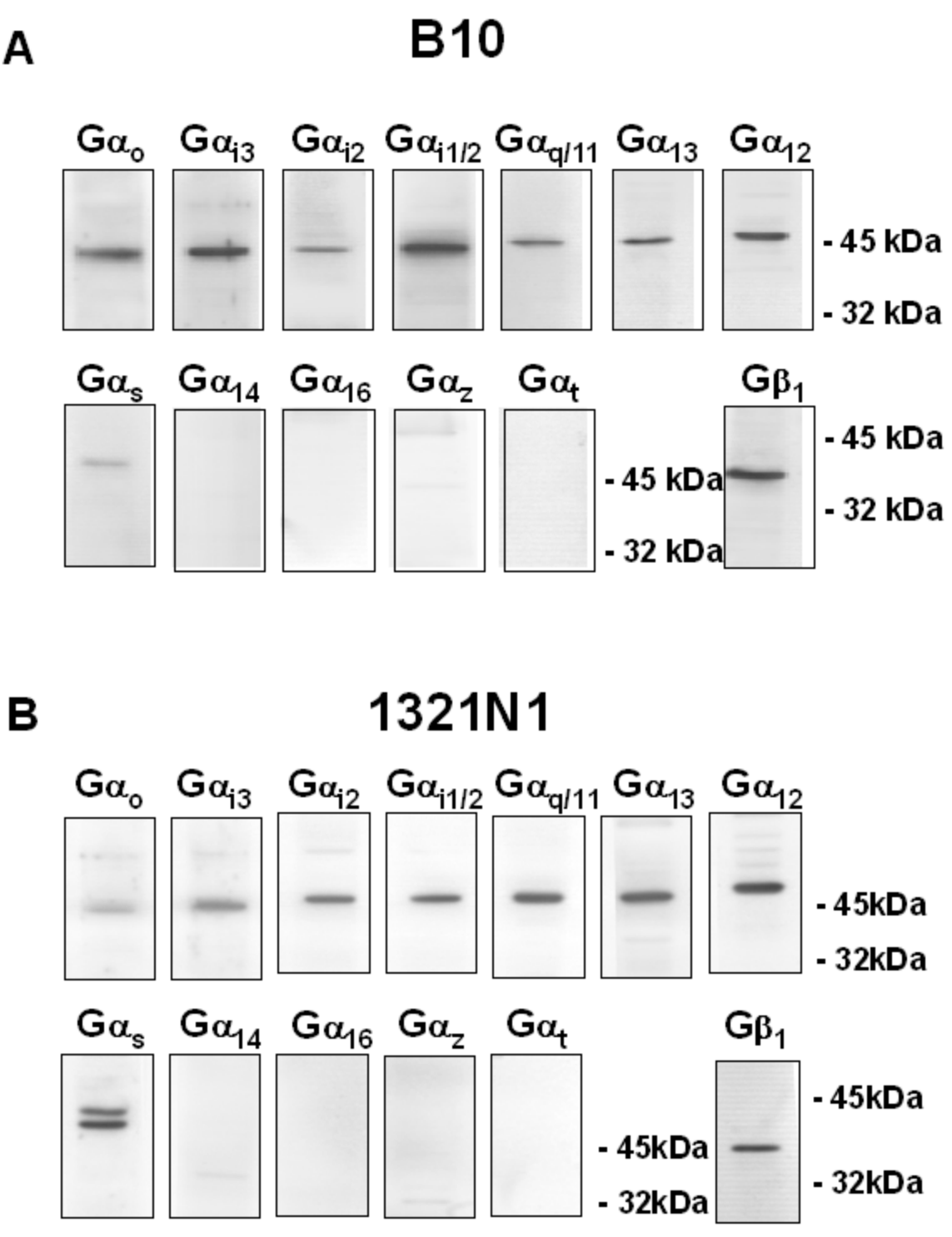
A
B10
Gαo
Gαi3
Gαi2
Gαi1/2
Gαq/11
Gα13
Gα12
- 45 kDa
- 32 kDa
Gαs
Gα14
Gα16
Gαz
Gαt
Gβ1
- 45 kDa
- 32 kDa
- 45 kDa
- 32 kDa
B
1321N1
Gαo
Gαi3
Gαi2
Gαi1/2
Gαq/11
Gα13
Gα12
- 45kDa
- 32kDa
Gαs
Gα14
Gα16
Gαz
Gαt
Gβ1
- 45kDa
- 32kDa
- 45kDa
- 32kDa

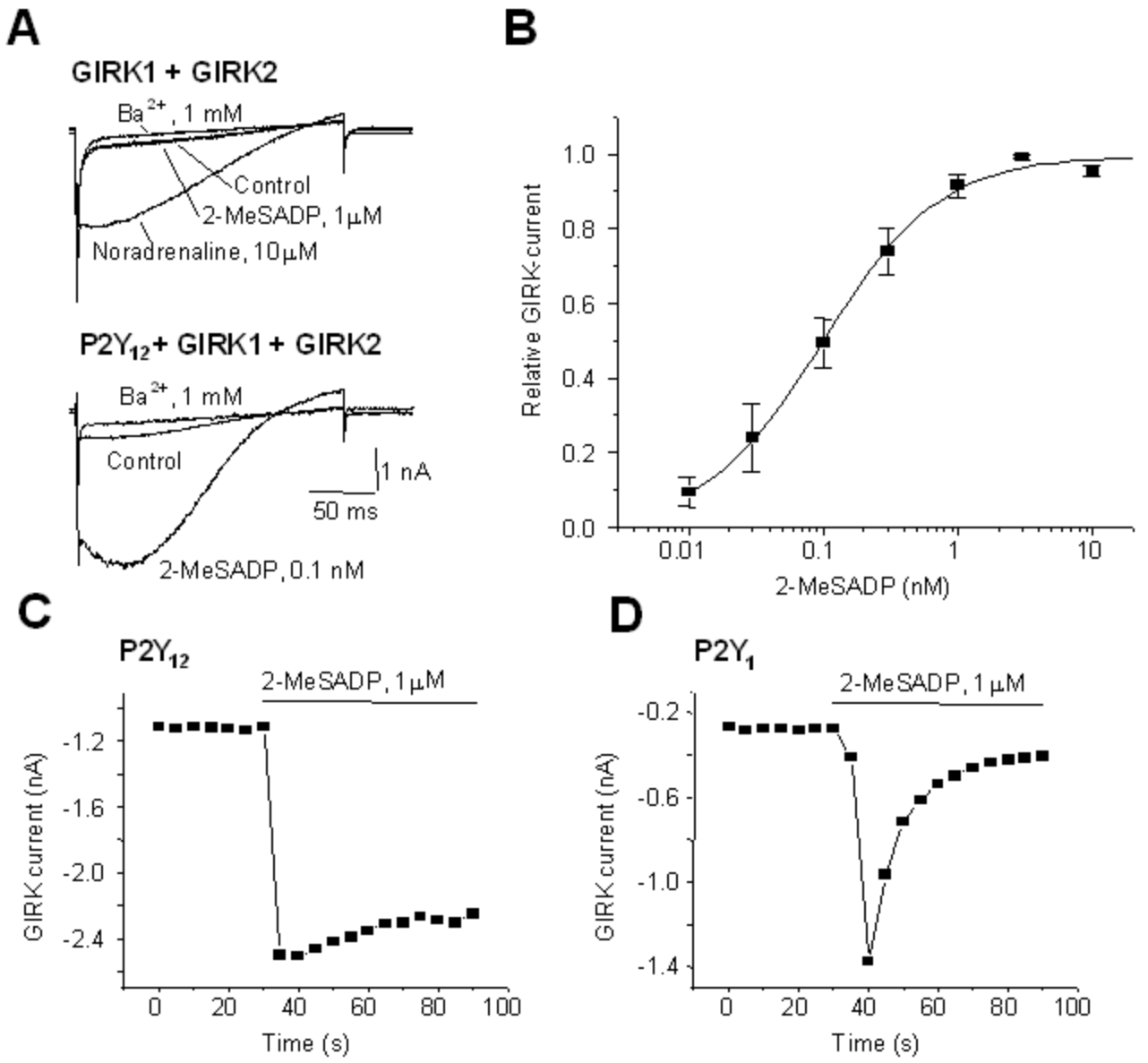
A
GIRK1 + GIRK2
Ba2+, 1 mM
Control
2-MeSADP, 1μM
Noradrenaline, 10μM
P2Y12+ GIRK1 + GIRK2
Ba2+, 1 mM
Control
1 nA
50 ms
2-MeSADP, 0.1 nM
B
Relative GIRK-current
1.0
0.8
0.6
0.4
0.2
0.0
0.01
0.1
1
10
2-MeSADP (nM)
C
P2Y12
2-MeSADP, 1μM
GIRK current (nA)
-1.2
-1.6
-2.0
-2.4
0
20
40
60
80
100
Time (s)
D
P2Y1
2-MeSADP, 1μM
GIRK current (nA)
-0.2
-0.6
-1.0
-1.4
0
20
40
60
80
100
Time (s)

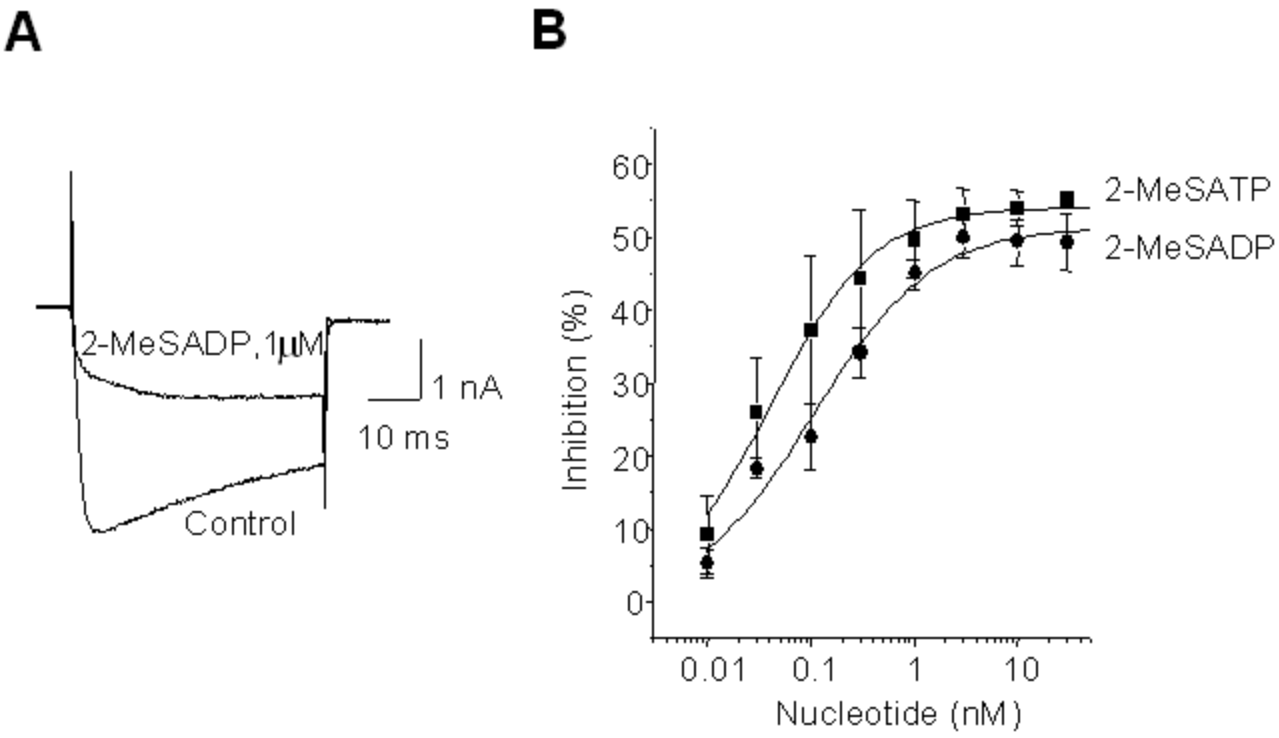
A
2-MeSADP, 1μM
1 nA
10 ms
Control
B
Inhibition (%)
60
50
40
30
20
10
0
0.01
0.1
1
10
Nucleotide (nM)
2-MeSATP
2-MeSADP

Simon *et al.*, Fig. 8

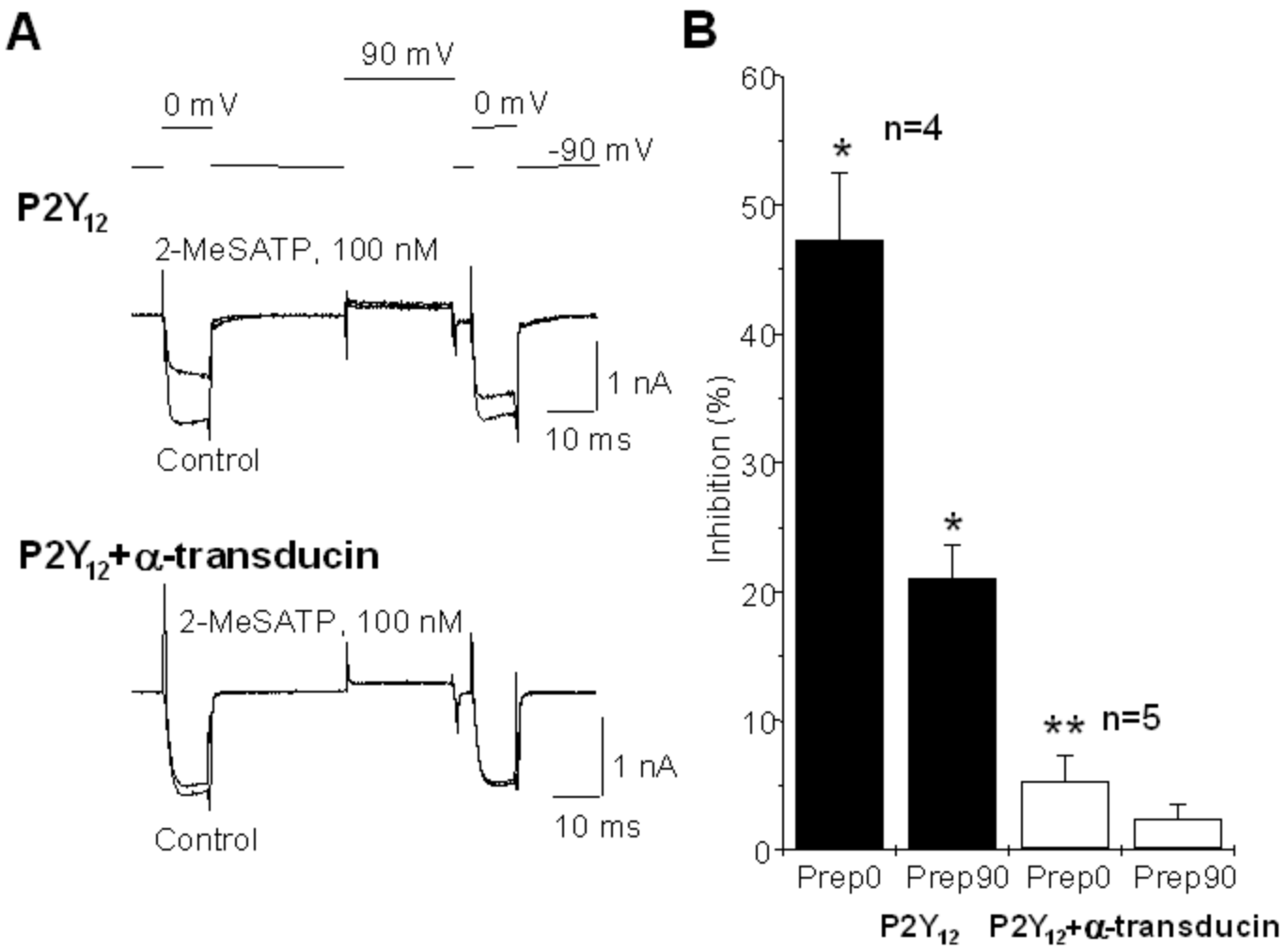

Characterization and channel coupling of the P2Y12 nucleotide receptor of brain capillary endothelial cells

Joseph Simon, Alexander K. Filippov, Sara Goransson, Yung H. Wong, Christian Frelin, Anton D. Michel, David A. Brown and Eric A. Barnard

J. Biol. Chem. published online June 21, 2002
